Effects on Fourier Peaks Used for Periodic Pattern Detection

Chun-Jung Tai [a] ***; Robert Ulichney*** [b] ***; Jan P. Allebach*** [a] ***;***
[a] ***Purdue University, West Lafayette, IN, U.S.A;*** [b] ***HP Labs, Stow, MA, U.S.A***

Abstract

The detection of quasi-periodic patterns, such as those found in clustered-dot halftones, can be efficiently achieved by searching for strong peaks in the frequency domain. In this paper, we quantify four factors that contribute to the attenuation of those characteristic peaks related to mobile hand-held image capture. These include MTF, halftone cluster size, blur, and contrast. We derive the expected theoretical attenuation for each of these factors, and then compare these with experimentally measured results from mobile captured images of test prints.

1. Introduction

Embedding data in hardcopy has a number of useful applications for which the image capture can be easily accomplished with mobile cameras. 1D and 2D barcodes are the most common means of embedding such data. Barcode readers require fiducial marks, such as the large concentric squares on three corners around a QR code that preprocessors use to detect the barcode [1]. Fiducial marks, and barcodes in general, are considered by many as perceptually ugly, particularly when used in documents.

A high capacity more aesthetically pleasing alternative to barcodes is embedding data in clustered-dot halftones. Methods include modulating the orientation of elliptical halftone dot clusters [2] or shifting the positions of the dot clusters [3]. While data-bearing halftones are more attractive than barcodes, the lack of fiducials can make camera-based detection more challenging. However, the quasi-periodic nature of these patterns affords very easy detection in the frequency domain [4]. The halftone patterns reveal four characteristic peaks in the Fourier Transform amplitude. The relative locations of these peaks also indicate to the decoder the orientation and scale of the halftone. As these frequency peaks are central to fast decoding, it is important to account for the things that can affect their amplitude. Knowing *a priori* the conditions that account for peak attenuation helps with the peak detection process. In addition, directly measuring peak attenuation can serve as an indicator of the quality of the captured image.

While there is considerable work in the area of image quality measurement, and particularly for mobile devices [5], the quantification of the factors that contribute to the collective attenuation of frequency peak amplitude has not been reported. Examining the details of Fourier peak attenuation for quasi-periodic patterns is the focus of this work. We organize the paper into two main parts. In the first part, we identify four of the most influential factors affecting peak amplitude, and derive the expected attenuation. In the second part, we compare this with experimental measurements using a mobile camera.

2. Four Peak Attenuation Factors

Our goal is to quantify each of the factors that contribute to the attenuation of characteristic peaks in the frequency domain. These include:
(1) Optical System MTF – the modulation transfer function is the magnitude response to sinusoids of different frequencies [6]. It is a measure that comes into play with pattern resolution and camera to object distance;
(2) Size of dot clusters – the size of the clusters that make up a halftone change as the gray level to be rendered varies from light to dark;
(3) Motion blur and focus – consequences of hand-held mobile devices; and
(4) Contrast – a measure characterizing the difference between the lightest and darkest part of the halftone pattern, resulting primarily from differences in illumination.

The next subsection will first define the periodic pattern that is of interest and its Fourier peak. The following subsections will then address each of the factors separately.

2.1 Peak of Periodic Pattern

In this section, we analyze the characteristics of the type of periodic pattern that is of interest in this paper. We assume that it consists of an array of dot clusters $d(x,y)$ that repeat on a square lattice with interval $X \times X$ within a square window with size $W \times W$. Thus, the image can be expressed as

$$f(x,y) = rep_{X,X}(d(x,y)) \cdot rect(\frac{x}{W}, \frac{y}{W}) \tag{1}$$

Define $F(u,v)$ as continuous space Fourier Transform (CSFT) of $f(x,y)$.

$$F(u,v) = (\frac{1}{X})^2 comb_{\frac{1}{X},\frac{1}{X}} D(u,v) ** W^2 sinc(Wu, Wv) \tag{2}$$

$$\approx (\frac{W}{X})^2 \sum_k \sum_l D(\frac{k}{X}, \frac{l}{X}) \delta(u - \frac{k}{X}, v - \frac{l}{X}) \tag{3}$$

Here $D(u,v)$ is the CSFT of the dot cluster $d(x,y)$. To obtain Equation (3) from Equation (2), we assume that $X \ll W$, i.e. that the $W \times W$ window contains a sufficient number of repetitions of the dot cluster $d(x,y)$.

Equation (3) shows that there will be strong localizations of energy in $F(u,v)$, at frequencies $(u,v) = (k/X, l/X)$, where k and l are integer-valued. In order to determine these locations digitally, we sample in the x and y directions at interval S, and compute the Discrete-Space Fourier Transform (DSFT) $F(\mu,\nu)$, where the frequency variables μ and ν have units in cycles/pixel. The spectrum $F(\mu,\nu)$ is of interest in the range $-0.5 < \mu, \nu < 0.5$, and the peaks indicated in Equation (3) will

occur at frequencies $(\mu,\nu)=(k/M,l/M)$, where $M=X/S$ is assumed to be integer-valued. We define the peak of the fundamental frequency as the maximum peak value which is not located on the μ or ν axis. More specifically,

$$\max(|F(\mu,\nu|\mu,\nu\neq 0)).=\max\left(|D\left(\pm\frac{k}{M},\pm\frac{l}{M}|k,l\neq 0\right)|\right) \tag{4}$$

To find the location of the maximum peak, we apply the method described in [3]. It will be convenient to normalize the maximum peak magnitude by the DC value $F(0,0)$ of the spectrum. In addition, we will be interested to study the behavior of the peak magnitude as the dimension of the dot cluster varies. So we define the normalized maximum peak magnitude as

$$P_m=\frac{max(|F(\mu,\nu)|)}{|F(0,0)|}, \text{ where } \mu,\nu\neq 0 \tag{5}$$

Here, m denotes the number of pixels in the dot cluster. In the remainder of this paper, we will drop the adjective *normalized* when referring to the peak magnitude. However, we will always mean normalized peak magnitude.

2.2 Optical System MTF

Among the effects that may change the image quality, the modulation transfer function (MTF) behaves as a low pass filter to decrease the magnitude of higher frequencies. We measured the MTF of our mobile device by using the (ISO 12233) slanted edge analysis tool with the (ISO 16067) QA-62 target. Figure 1 was measured on an iPhone 5 by the slant edge method. The MTF curve provides an understanding of how much the peak is attenuated for periodic objects with different repetitive frequencies.

An awareness of the MTF effect is important because the fundamental peak does not occur at a fixed location. The magnitude of the fundamental peak is decided by how close the camera is to the target, as well as the resolution at which the target has been printed. Depending on the combination of the printing resolution and camera resolution, the location of the peak value changes significantly. The peak will suffer MTF attenuation even if the camera is perfectly focused and still. Theoretically, if the fundamental peak is perfectly taken at frequency f_p, the peak value will be

$$P_{m,MTF}(f_p)=MTF(f_p)\frac{|P_m(f_p)|}{|P_m(0,0)|} \tag{6}$$

2.3 Size of Dot Clusters

The dot cluster size also affects the peak magnitude. In this section, we will use ideal digital images to show the peak magnitude for both 1D and 2D cases. An analysis will be provided to understand the theoretical maximum peak attenuation in the 1D case.

Assume the 1D highlight dot clusters shown in Figure 2(a) with period X inches and the dot cluster width mS inches, where as before, S is the sampling interval. Thus, each cluster contains m pixels. Let the black value of the dot cluster be 0, and the rest is 1. The 1D highlight dot cluster is given by

$$d_{m,1D}(x)=1-rect(\frac{x}{mS}) \tag{7}$$

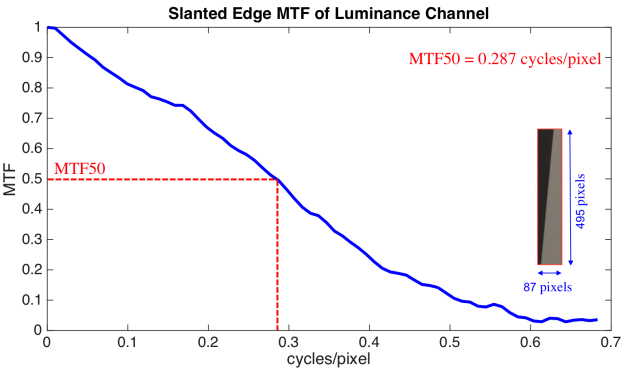

Figure 1: MTF measured on an iPhone 5 by slant edge analysis tool with (ISO 16067) Q-62 target. The cropped image on the right shows the vertical slanted edge being used.

Define $D_{m,1D}(u)$ as the 1D CSFT of $d_{m,1D}(x)$.

$$D_{m,1D}(u)=\delta(u)-mS\cdot sinc(mSu) \tag{8}$$

As we did in Section 2.1, we next consider the digital equivalent $d_{m,1D}[i]=d_{m,1D}(iS)$ of the 1D Continuous-Space (CS) dot cluster function. Here i is our spatial index. We then have for the absolute value of the DSFT of the dot cluster function

$$D_{m,1D}(\mu)=e^{-j\pi(M-1)\mu}\frac{sin(\pi M\mu)}{sin(\pi\mu)}-e^{-j\pi(m-1)\mu}\frac{sin(\pi m\mu)}{sin(\pi\mu)} \tag{9}$$

Here, as before, $M=X/S$ is the number of samples per period of the dot pattern. We define a 1D array $f_{m,1D}$ that consists of an array of dot clusters $d_{m,1D}$ that repeats with interval X with total length W. Thus the 1D signal $f_{m,1D}$ can be expressed as

$$f_{m,1D}(x)=rep_X(d_{m,1D}(x))\cdot rect(x/W) \tag{10}$$

Define $F_{m,1D}$ as the 1D CSFT of $f_{m,1D}$. Then

$$F_{m,1D}(u)=\frac{1}{X}comb_{\frac{1}{X}}D_{m,1D}(u)*Wsinc(Wu) \tag{11}$$

$$\approx\frac{W}{X}\sum_k D_{m,1D}(\frac{k}{X})\delta(u-\frac{k}{X}) \tag{12}$$

To calculate the peak attenuation in the 1D case, we use the normalized peak magnitude defined in Section 2.1. The 1D form of the maximum peak to DC value is

$$P_{m,1D}(f_{p,1D})=\frac{\max(|F_{m,1D}(\mu|\mu\neq 0)|)}{|F_{m,1D}(0)|} \tag{13}$$

$$=\frac{|m\cdot\sin(\pi m/M)|}{(M-m)|sin(\pi/M)|} \tag{14}$$

Here, we have used the fact that the maximum peak is located at $\mu=1/M$. We substitute μ in Equation (13) with $1/M$ to get Equation (14). Figure 2(b) shows that for a fixed period $M=8$ pixels, the peak magnitude gradually increases as the dot cluster m increases from size 1 to 4.

For the 2D case, the size of the clusters is defined by a dithering template [3] shown in Figure 3(a). The cluster is periodic and repeats every 8×8 pixels. Similar to the 1D case, the peak magnitude for a cluster with size m pixels is the value of the largest

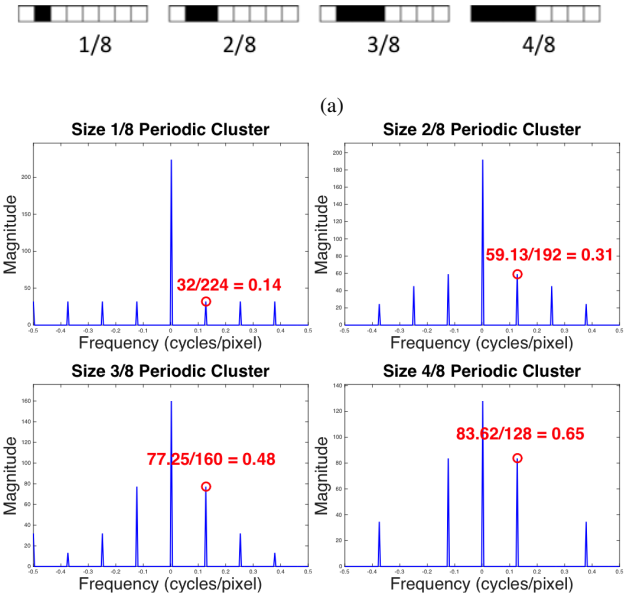

Figure 2: Relationship between peak spectral magnitude and 1D cluster width. (a) Cluster sizes 1 to 4. From left to right are non-periodic clusters with width 1/8, 2/8, 3/8, 4/8. (b) The DFTs of the corresponding periodic patterns.

peak to DC ratio denoted as $P_m(f_{p,2D})$ which occurs at frequency $f_{p,2D} = (\mu_p, \nu_p)$. We shorten $f_{p,2D}$ to f_p in the rest of paper. Unlike the 1D case, P_m is not monotonically increasing or decreasing from cluster size 1 to 16. The peak magnitude gradually increases as m increases from 1 to 16; but it decreases a little at cluster sizes 12 and 16 as indicated by the red line in Figure 3(b). This is caused by the asymmetric shape of the clusters along the x and y axes. However, if we take the peak magnitude to be the average of the magnitudes of the two largest peaks, this value will increase monotonically as the size of the dot cluster increases.

Figure 3(b) shows the peak magnitude for each size of highlight dot cluster in the 2D case. All peak magnitudes are normalized by the peak magnitude for the size 16 dot cluster. The blue line in Figure 3(b) shows the average peak magnitude of the maximum peak and second maximum peak for the indicated frequency range. In this case, the size 16 dot cluster has the maximum peak magnitude; and the size 1 dot cluster has the minimum peak magnitude.

2.4 Motion Blur and Focus

Blurriness would attenuate the peak magnitude. However, we want to find another metric that helps to identify image quality. The new quality metric does not search for the peak magnitude, but looks at the frequencies higher than the fundamental peak. We present two different image quality metrics largely based on features in the frequency domain. The two metrics we propose for quantifying quality are

(1) Q_E: a metric that measures the mean spectral magnitude at high frequencies;

(2) Q_{σ^2}: a metric that measures the variance in the spectral magnitude at high frequencies.

The introduction of blurriness to the image will increase

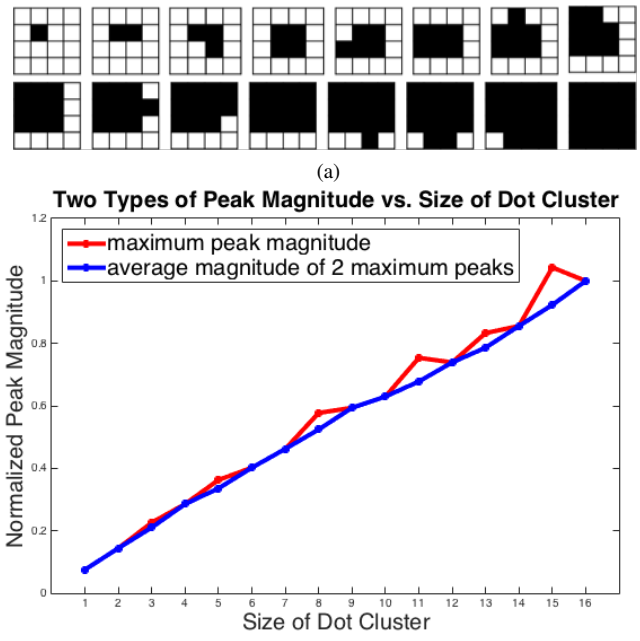

Figure 3: Relationship between peak 2-D DSFT spectral magnitude and 2D cluster area. (a) 2D highlight cluster sizes 1 to 16. The shape of the cluster is defined by [3]. Row one shows dot cluster sizes 1 to 8. Row two shows dot cluster sizes 9 to 16 (left to right). (b) Peak magnitude versus size of dot cluster. We use the highlight clusters defined in (a). The red line shows the maximum peak magnitude for the frequencies $-0.5 < \mu < 0.5, 0 < \nu < 0.5$. The blue line shows the normalized average peak magnitude of the two maximum peaks for the frequencies $-0.5 < \mu < 0.5$, $0 < \nu < 0.5$.

the energy at low frequencies and attenuate the peak at the fundamental frequency. The two quality metrics Q_E and Q_{σ^2} observe the mean and variance values at high frequencies, which may indicate the blurriness of the periodic image. From Equation (3), the higher frequency part of the periodic pattern CSFT spectrum will only have some smaller peaks located at frequencies $(u,v) = (k/X, l/X)$, where k and l take on integer values, and at least one of them must be greater than 1 in absolute value. The rest of the spectrum should have values close to 0. When blurriness is introduced to the image, energy is shifted to the low frequency part of the spectrum which reduces the mean and variance in high frequency part of the spectrum.

To examine this property, we define the two quality metrics mentioned at the beginning of this subsection. To align more closely with the calculations that are to be performed, we define these metrics in terms of the DSFT frequencies (μ, ν). We first define the frequencies above r as a set Ω_r.

$$\Omega_r = \{(\mu,\nu) | \sqrt{\mu^2+\nu^2} > r, 0.5 < \mu, \nu < 0.5\} \tag{15}$$

The set Ω_r is illustrated by the grey area shown in Figure 4. Here, we specifically choose the radius r so that Ω_r does not include the peaks corresponding to the fundamental frequencies of the periodic pattern. The area of Ω_r is denoted as A_r.

$$A_r = 1 - \pi r^2 \tag{16}$$

We define E_r as the sum of the spectral magnitude $|F(\mu,\nu)|$ in Ω_r; and we define Q_E and Q_{σ^2} according to,

$$Q_E = E_r/F(0,0) \tag{17}$$

$$Q_{\sigma^2} = \frac{\sum_{(\mu,\nu)\in\Omega_r} (|F(\mu,\nu)| - \frac{E_r}{A_r})^2}{A_r \cdot (F(0,0))^2} \tag{18}$$

As indicated above, Q_E and Q_{σ^2} are both functions of r which determines the range of high frequencies. For our testing image, we perform a search for the radius r which yields the maximum value for Q_{σ^2}.

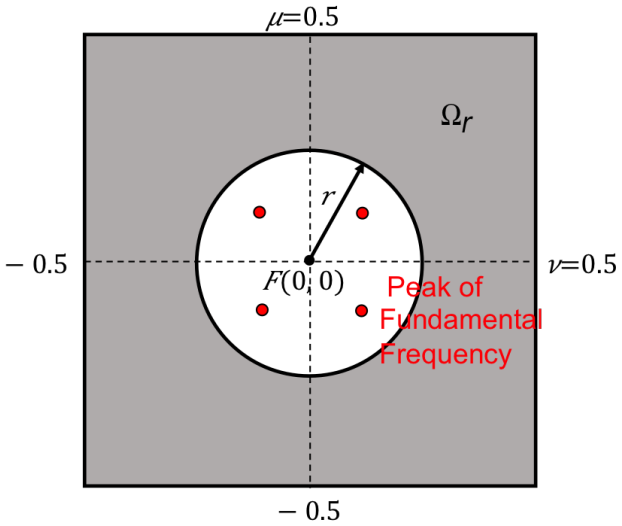

Figure 4: Illustration of high frequency region Ω_r used to calculate the quality metrics Q_E and Q_{σ^2}.

2.5 Contrast

Image contrast affects the binary image by reducing the difference between the grey values of the black and white colors. Cameras, just like human eyes, are sensitive to image contrast. When the contrast is reduced, the difference between the black and white colors becomes more difficult to distinguish. Contrast is another factor that would affect the peak magnitude. In order to study the effect of contrast, we first define $f_0(x,y)$ as the periodic pattern of full-range-contrast dot clusters $d_0(x,y)$ that repeat on a square lattice with interval $X \times X$ within a square window with size $W \times W$, where the grey value of a black dot is 0 and the rest of the area is 1.

Let $d(x,y)$ be the imperfect version of dot cluster $d_0(x,y)$, where the black and white values of the dot cluster are shifted so the contrast is reduced. We define $f(x,y)$ as the periodic pattern of dot clusters $d(x,y)$ that repeats on the square lattice with interval $X \times X$ inches within a square window with size $W \times W$ inches. As before, we sample $f(x,y)$ with interval S inches to represent $f(x,y)$ digitally, where $M = X/S$ and $N = W/S$ are assumed to be integer-valued. We use the luminance contrast to define the sensitivity to change in grey level. The luminance contrast is given by

$$\lambda = \frac{\max f - \min f}{\text{average}(f)} = \frac{\max f - \min f}{\frac{1}{N^2}\sum_{i=0}^{N-1}\sum_{j=0}^{N-1} f[i,j]} = \frac{\max f - \min f}{\frac{1}{N^2}F(0,0)}, \tag{19}$$

where $F(0,0)$ is the DC value of the DSFT of $f[i,j]$. We can also write Equation (19) in terms of the dot cluster function $d[i,j]$.

$$\lambda = \frac{\max d - \min d}{\frac{1}{N^2}(\frac{N}{M})^2 \sum_{i=0}^{M-1}\sum_{j=0}^{M-1} d[i,j]} = \frac{\max d - \min d}{\frac{1}{M^2}\sum_{i=0}^{M-1}\sum_{j=0}^{M-1} d[i,j]}, \tag{20}$$

We define $\gamma = \min d$ and $\xi = \max d - \min d$. The contrast λ is

$$\lambda = \frac{\xi}{a\cdot(\gamma+\xi)+b\cdot\gamma} \tag{21}$$

where $1/2 < a < (x^2-2)/x^2$ and $b = 1-a$ for a highlight dot cluster. Here a and b are the ratio of the areas covered by white and black color, which depends on the size of the highlight dot cluster. In general, $a \neq b$. For example, the size 4 highlight dot cluster shown in Figure 3(a) is covered by $a = 7/8$ white and $b = 1/8$ black. The ratio of the peak magnitude to the contrast that was derived in Equation (19) is

$$\frac{P_m}{\lambda} = \frac{F(f_p)}{F(0,0)}\left(\frac{1/N^2 \cdot F(0,0)}{\max f - \min f}\right) \tag{22}$$

Next, we replace $f(x,y)$ in terms of $f_0(x,y)$. That is $f(x,y) = \xi f_0(x,y) + \gamma$. As before, for purpose of computation, we work with the sampled versions of these functions. The DFT $F[k,l]$ of $f[i,j]$ is given by

$$F[k,l] = \xi F_0[k,l] + \gamma\delta[k,l], \text{ where } k,l = 0,\ldots,M-1 \tag{23}$$

Here $\delta[k,l]$ denotes the 2D unit sample function, which has value 1 for $(k,l) = (0,0)$ and value 0, otherwise. Then,

$$F[k,l] = \begin{cases} \xi F_0[k,l] & \text{, for } k \neq 0, \text{ or } l \neq 0 \\ \xi + \gamma & \text{, for } k,l = 0 \end{cases} \tag{24}$$

Because $f_p \neq (0,0)$, Equation (22) can be written as

$$\frac{P_m}{\lambda} = \frac{1/N^2(\xi F_0(f_p))}{\xi} = \frac{F_0(f_p)}{N^2} \tag{25}$$

$F_0(f_p)$ and N^2 are the same for different contrast levels. Thus, equation (25) shows that the peak-magnitude-to-contrast ratio is a constant.

3. Experimental Results

To study the four quality factors that affect the peak in the Fourier spectrum of a periodic pattern, we designed the following experiment which will be explained in Sections 3.1 through 3.4. All experimental images are printed by HP LaserJet monochrome printers and captured by the back camera on an iPhone 5.

3.1 Optical System MTF

We designed a test page to examine the influence of the optical system MTF on the peak magnitude in the Fourier spectra of periodic patterns with different fundamental frequencies. In order to minimize the the effect of digital camera image processing (i.e., auto white balance, auto exposure), all the periodic patterns with different fundamental frequencies should be captured in one shot. This will allow the same image processing adjustment by the camera to all the periodic patterns. The test page for measuring MTF attenuation is designed as a set of samples with gradually increasing periodic frequency. We use a size 4 dot cluster. In other words, the period M changes from sample-to-sample. We designed a test page with 8 samples with gradually increasing periodic M. We shot the test page under conditions such that the illumination was the same over the entire the test page.

The experimental results are shown in Figure 5. Figure 5(a) shows the peak magnitude for the different samples. To obtain an accurate estimate of the peak magnitude from the entire sample, we randomly cropped each sample into five 128×128 pixels patches, computed the DFT of each patch, and averaged the peak magnitudes over the five cropped patches. We normalized each peak magnitude to 1 by dividing it by the peak magnitude of the lowest fundamental frequency patch among all the samples.

Figure 5(a) shows that the peak attenuation becomes more serious when the fundamental peak moves to a higher frequency. The peak magnitude is attenuated to nearly zero when the frequency of the fundamental peak is above 0.2 cycles/pixels, in which case the period of the dot clusters is 5 pixels. The lowest frequency that we measured in this experiment is 0.05 cycles/pixel, which corresponds to a period of 20 pixels. We conjecture that for longer periods, the fundamental frequency in the periodic pattern may be masked by noise in the vicinity of origin of the spectrum of the periodic pattern. From our experiments, the range of the fundamental peak location that is able to be captured by the camera is roughly from 0.05 to 0.33 cycles/pixels.

Compared to the camera MTF curve measured in Figure 1, the peak in the Fourier spectrum of the printed and camera-captured periodic pattern has a narrower range of fundamental frequencies that can be used with dot cluster size 4. Comparing our peak magnitude measurements with the optical system MTF, we observe that both the peak magnitude and the MTF decrease with increasing frequency.

3.2 Size of the Dot Cluster

In Section 2.3, we showed that the peak magnitude depends on cluster size. To test the peak attenuation caused by cluster size, we designed a test page with patches that have different cluster sizes. For the same reason we mentioned in Section 3.1, all the patches are captured in one shot with similar illumination over the entire image to minimize the variation of the camera signal processing. We randomly cropped fifteen 128×128 pixels samples from each patch of dot clusters, and computed the average of peak height. Example of two cropped samples are shown in Figure 6(a).

In this experiment, all clusters size patterns are captured at the same fundamental frequency; so the MTF should attenuate the peaks equally. However, different cluster sizes would not have the same contrast value. This can be explained by the Murray-Davies dot gain equation. This will further attenuate the peak magnitude

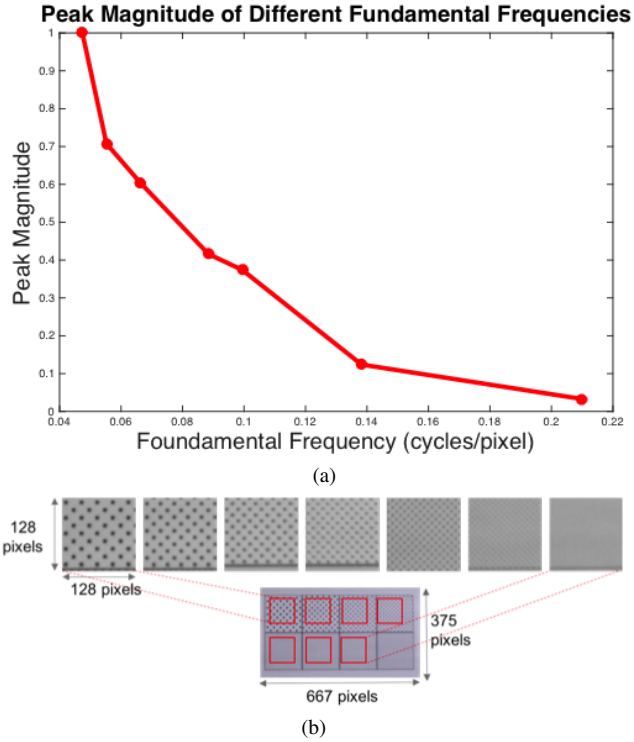

Figure 5: Effect of optical system MTF on Fourier spectrum peak magnitude. (a) Peak magnitude for six different fundamental frequencies corresponding to the periodic patterns shown in (b) from left to right with image size 128×128 pixels.

of the smaller sized dot clusters due to the low contrast. We can observe this in Figure 6(a). The size 1 cluster pattern is lighter than the size 16 cluster pattern.

The experimental result is shown in Figure 6(b). The peak height is defined as the average magnitude of the two maximum peaks. We normalized the peak magnitude by dividing it by the peak magnitude of size 16 dot cluster. We use the red dashed line to show the peak magnitude from the digital cluster, and use the blue solid line to show the experimental peak magnitude. It is shown that the camera captured peak magnitude generally agrees with the digital sample. However, the peak magnitudes for the camera-captured dot-clustered patterns do not monotonically increase with the size of the dot cluster. The pattern for cluster size 16 has the largest peak magnitude; and the pattern for size 1 dot cluster has the smallest peak magnitude.

3.3 Motion Blur and Focus

We have defined two quality metrics in Section 2.4 to check the mean and variance of the high frequency content. In this section, the two quality metrics are examined with a set of images. We first grouped the images into three quality levels, bad, fair and good according to the following criteria. In the good level, dot clusters are clearly separated with clean boundaries between black and white values. The size and shape of dot clusters may be hard to recognized, but clean boundaries can be observed. For images categorized to the good level, they are recommended for further processing, such as image alignment or decoding the embedded data. For the fair level, the boundaries of dot clusters are blurry, but each cluster is still separated. The observer can distinguish the

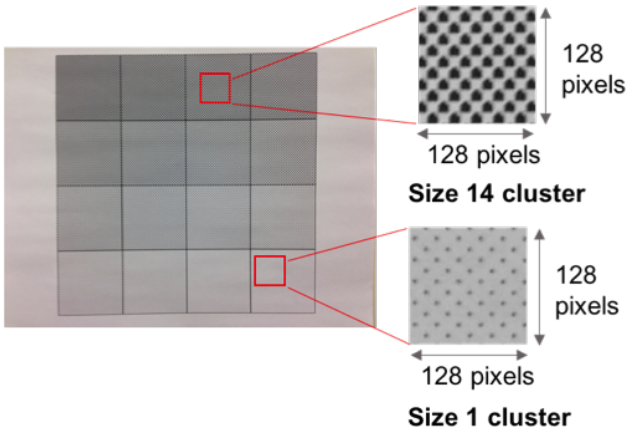

(a)

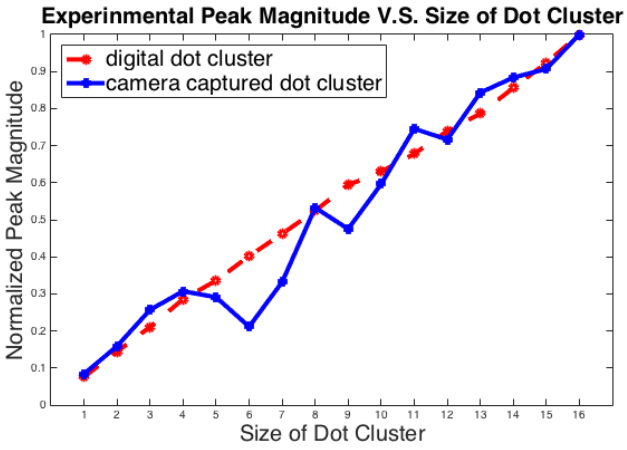

(b)

Figure 6: Effect of size of dot cluster to peak magnitude on the camera-captured image. (a) Example of a cropped sample of size 1 cluster and a size 14 cluster from camera-captured image. (b) Digital peak magnitude is shown in red dashed line. Camera-captured peak magnitude is shown in blue solid line.

width of periodic dot clusters. The quality of the fair level may be the result of camera lens movement or hand shaking when the image is captured. Such video frames can be used for further decoding, but we can expect the decode accuracy to decrease. For the bad level, the clusters are not separated and strong blurriness due to motion or improper focus can be observed. These images are not recommended for further processing.

Figure 7 shows examples of the three quality levels. We captured video on the same object with 56 frames in total. The object contains all sizes of dot cluster. We cropped a 256×256 pixels window from every frame at the same location, and categorized every video frame to one of the three quality levels. To capture our video samples, we first wait for the camera to focus then slightly shake the camera to blur the video. We then stop shaking the camera and wait for the camera to refocus. Because the video frame is continuous, the quality level will be consistent at neighboring frames. For example, frames 1 to 10 in our experimental video are categorized to the quality level fair. Frames 11 to 25 are categorized to the quality level good. Frames 28 to 32 are categorized to the quality level bad.

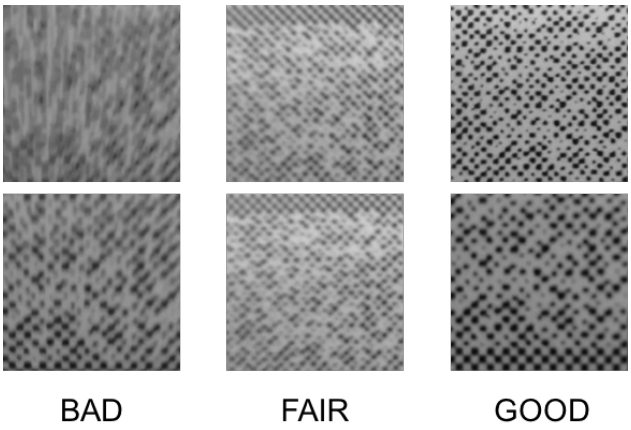

Figure 7: Three different image quality levels of periodic patterns. Columns from left to right show image quality level from bad to good. The object is a periodic dot cluster pattern with mixing cluster sizes.

To compare the three categories with the quality metrics, we use the two quality metrics Q_E and Q_{σ^2} from Equation 17 and 18. The experimental result is shown in Figure 8. Figure 8(a) uses the quality metric Q_E to measure the quality levels and Figure 8(b) uses the quality metric Q_{σ^2} to measure the quality levels. Our results show that the quality metrics Q_E separates the three quality levels better than Q_{σ^2}.

3.4 Contrast

To study contrast, we generated two types of test pages. The Type 1 patches fix the middle grey value, and shift the black and white value equally toward the middle value. The Type 2 patches fix the black value, and shift the white value toward the black value. Figure 9 shows the camera-captured images of the two types of contrast. The image is captured in one shot. Theoretically, Type 2 contrast has the minimum grey value γ fixed to zero. Equation (20) shows when $\gamma = 0$, contrast is equal to $1/a$ regardless of how much the white value is shifted. However, this will not happen in the real scenario, since the minimum grey level will not be zero under sufficient lighting. If the minimum grey level is nearly zero, the entire picture is most likely taken in very low light condition and the entire target may not be seen.

To measure the relationship between contrast and peak magnitude on the camera-captured images, we randomly crop fifteen 128×128 pixels samples from the each of the patches as shown in Figure 9. The measured contrast versus peak magnitude is depicted in Figure 10. Each dot represents the measurement from a cropped sample. For the ideal periodic dot cluster, Equation (25) shows that the peak magnitude to the contrast is a constant. For the experimental results, 160 samples of Type 1 and Type 2 are fitted onto a straight line. Our result shows that the peak magnitude increases with the contrast.

4. Conclusion

In this paper we quantify four factors that contribute to the attenuation of the characteristic peaks related to mobile hand-held image capture of periodic clustered-dot halftone patterns containing embedded metadata. These include blur, MTF, halftone cluster size, and contrast. We first used a theoretical approach based

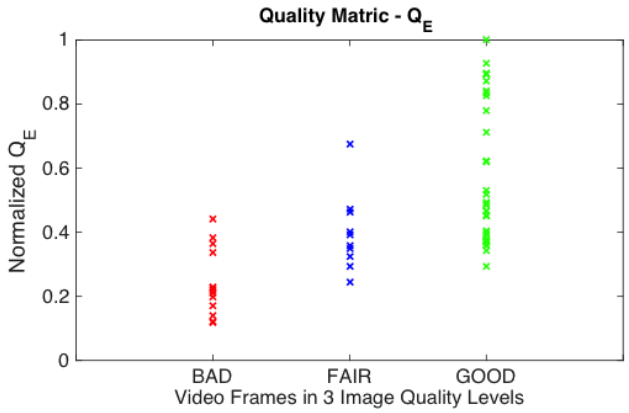

(a)

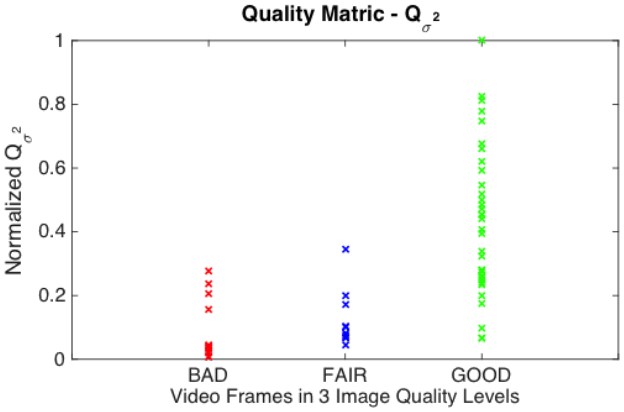

(b)

Figure 8: Quality metrics tested on 56 continuous video frames. We first group the video frames into three quality levels by the rules defined in Section 3.3. Then, we calculate the image quality by the two quality metrics. Green dots are frames with good quality. Blue dots are frames with fair quality. Red dots are frames with bad quality. (a) and (b) show the results of quality metric Q_E and Q_{σ^2}.

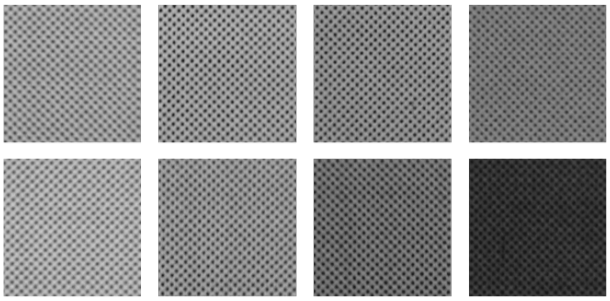

Figure 9: Two types of contrast being captured by camera. The upper row shows Type 1 contrast. The lower row shows Type 2 contrast.

on ideal digital images to discuss the four factors. An experiment was then conducted to verify the four factors using digital images captured with a camera. A comparison between theoretical values and experimental values were made for each of the factors.

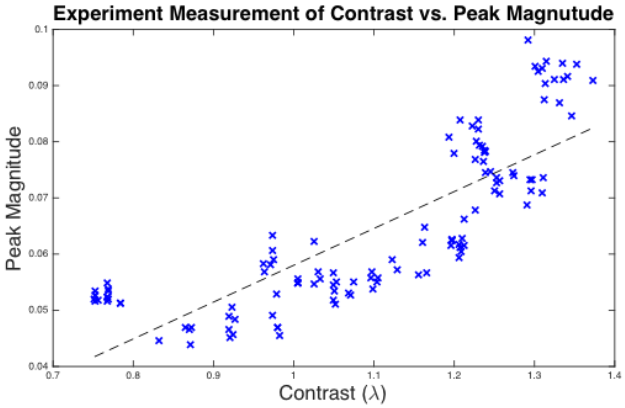

Figure 10: Relationship of the contrast to the peak magnitude computed from 160 samples of Type 1 and 2 patches. The sample points are fitted onto a straight line.

References

[1] Eisaku Ohbuchi, Hiroshi Hanaizumi, and Lim Ah Hock, "Barcode readers using the camera device in mobile phones," in *Cyberworlds, 2004 International Conference on*. IEEE, 2004, pp. 260–265.

[2] Orhan Bulan, Vishal Monga, Gaurav Sharma, and Basak Oztan, "Data embedding in hardcopy images via halftone-dot orientation modulation," in *Electronic Imaging 2008*. International Society for Optics and Photonics, 2008, pp. 68190C–68190C.

[3] Robert Ulichney, Matthew Gaubatz, and Steven Simske, "Encoding information in clustered-dot halftones," in *NIP & Digital Fabrication Conference*. Society for Imaging Science and Technology, 2010, vol. 2010, pp. 602–605.

[4] Robert Ulichney, Stephen Pollard, and Matthew Gaubatz, "Fast mobile stegatone detection using the frequency domain," in *NIP & Digital Fabrication Conference*. Society for Imaging Science and Technology, 2014, vol. 2014, pp. 237–242.

[5] Veli-Tapani Peltoketo, "Signal to noise ratio and visual noise of mobile phone cameras," *Journal of Imaging Science and Technology*, vol. 59, no. 1, pp. 10401–1, 2015.

[6] Glenn D Boreman, *Modulation transfer function in optical and electro-optical systems*, vol. 4, SPIE Press Bellingham, WA, 2001.

Author Biography

Chun-Jung Tai received her BS in Electrical and Computer Engineering from the National Chiao Tung University, Hsinchiu, Taiwan (2011). She is currently pursuing her PhD degree in Electrical and Computer Engineering at Purdue University, West Lafayette, IN, USA. She interned with HP Labs from 2012 to 2014. During this time, she completed the work reported in this paper.

Robert Ulichney is a Distinguished Technologist with HP Labs focusing on systems for high capacity data embedding, and structures for variable density 3D printing. He received a Ph.D. from MIT in Electrical Engineering and Computer Science. Before joining HP, he was with Digital Equipment Corp for several years then with Compaq's Cambridge Research Lab, where he led a number of research projects on image and video implementations for both hard copy and display products.

Jan P. Allebach is Hewlett-Packard Distinguished Professor of Electrical and Computer Engineering at Purdue University. Allebach is a

Fellow of the IEEE, the National Academy of Inventors, the Society for Imaging Science and Technology (IS&T), and SPIE. He was named Electronic Imaging Scientist of the Year by IS&T and SPIE, and was named Honorary Member of IS&T, the highest award that IS&T bestows. He has received the IEEE Daniel E. Noble Award, and is a member of the National Academy of Engineering. He currently serves as an IEEE Signal Processing Society Distinguished Lecturer (2016-2017).